Original Article

Genipin protects against mitochondrial damage of the retinal pigment epithelium under hyperglycemia through the *AKT* pathway mediated by the *miR-4429/JAK2* signaling axis

Wenshuang Xu[1], Qingyou Chen[2], Xiaofeng Zhang[3], Yue Zhao[3], Shuang Wu[4], Chao Yang[4], Yubao Liu[5], Lijie Liang[6], Di Jia[4], Chaojun Li[4], Li Fan[4], Yan Shi[4]

[1]Department of Ophthalmology, Qiqihar Eye & ENT Hospital, Qiqihar, China; [2]Department of Neurology, The Third Affiliated Hospital of Qiqihar Medical University, Qiqihar, China; [3]Department of Ophthalmology, The First Hospital of Qiqihar, Qiqihar, China; [4]College of Medical Technology, Qiqihar Medical University, Qiqihar, China; [5]Department of Intensive Care Unit, The Second Affiliated Hospital of Qiqihar Medical University, Qiqihar, China; [6]Department of Ultrasound, The Second Affiliated Hospital of Qiqihar Medical University, Qiqihar, China

Contributions: (I) Conception and design: Y Shi, W Xu; (II) Administrative support: Q Chen, C Li; (III) Provision of study materials or patients: X Zhang, Y Zhao, Y Liu, L Liang; (IV) Collection and assembly of data: S Wu, C Yang; (V) Data analysis and interpretation: D Jia, L Fan; (VI) Manuscript writing: All authors; (VII) Final approval of manuscript: All authors.

Correspondence to: Yan Shi. College of Medical Technology, Qiqihar Medical University, No. 333, Bukui Street, Jianhua District, Qiqihar 161006, China. Email: shiyan202161@163.com.

Background: To investigate the protective effect and mechanism of genipin (GE) on mitochondrial damage in retinal pigment epithelial (RPE) cells induced by high glucose.

Methods: Differential genes of GE in the treatment of diabetic retinopathy (DR) were screened by the Gene Expression Omnibus (GEO) database. Differential genes located in the *AKT* pathway were obtained. TargetScan, miRDB, and DIANA databases were used to predict the targeted microRNAs (miRNAs) of differential genes. A high-fat diet combined with streptomycin (STZ) intraperitoneal injection were used to establish a diabetic mouse model. Diabetic mice were treated with GE by intragastric administration. The functional and molecular changes of the retina were detected by electroretinogram (ERG) and reverse transcription-polymerase chain reaction (RT-PCR). ARPE-19 cells were cultured under hyperglycemic conditions with *AKT* and *JAK2* inhibitors. *MiR-4429* was knocked down/overexpressed to detect changes in cell function, activity, and mitochondrial function. The dual luciferase reporter assay confirmed the targeted binding of *miR-4429* with *JAK2*.

Results: Bioinformatics analysis finally yielded *JAK2* as the research target gene. *miR-4429* was predicted to be the targeted miRNA of *JAK2* by online databases. The results of animal experiments showed that the retinal function of mice recovered after GE administration ($P<0.05$), the expression of *AKT* and *miR-4429* in RPE cells was significantly increased ($P<0.05$), and the expression of *JAK2* was significantly decreased ($P<0.05$). The results of cell experiments showed that the functions of cells and mitochondria recovered after the addition of GE under hyperglycemia ($P<0.05$). Cell and mitochondrial functions were decreased after the addition of *AKT* inhibitor ($P<0.05$). Overexpression of *miR-4429* or inhibition of *JAK2* increased cell activity and mitochondrial function ($P<0.05$). The results of the dual luciferase reporter assay showed that *miR-4429* had a targeted binding site with *JAK2*.

Conclusions: GE protects ARPE-19 cell functional activity, inflammatory responses, and mitochondrial damage by promoting the *AKT* signaling pathway and regulating the expression of the *miR-4429/JAK2* signaling axis.

Keywords: Genipin (GE); *AKT*; *miR-4429*; *JAK2*; retinal pigment epithelial (RPE)

Submitted Apr 13, 2022. Accepted for publication May 20, 2022.

doi: 10.21037/atm-22-2219

View this article at: https://dx.doi.org/10.21037/atm-22-2219

Introduction

As a common microvascular complication of diabetes, diabetic retinopathy (DR) is the main cause of vision loss in diabetic patients (1). A study has shown that in 2017, the total number of patients diagnosed with DR was about 93 million, among which about 28 million had visual impairment due to retinopathy (2). DR is a special diabetic microvascular complication. Through epidemiological studies in many places in China, it has been found that people with DR will be accompanied by low vision and even blindness. At present, it has become one of the main causes of blindness. Therefore, how to effectively treat DR to reduce the risk of blindness is particularly important.

Current scientific research is trying to find targets for DR through mechanistic studies so as to treat DR efficiently via these targets. As an important part of retinal tissue, retinal pigment epithelial (RPE) cells are closely related to the occurrence and development of DR (3). An anatomical study has shown that the retinal pigment epithelium is mainly located in the lower layer of the retina and consists of a single layer of cells (4). Its main functions are supporting photoreceptor cells, regulating blood transport and humoral conversion, and visual pigment synthesis and regeneration. Therefore, the retinal pigment epithelium plays an important role in the maintenance of the retinal microenvironment (5). In diabetic patients, due to microvascular disease, the blood supply of retinal tissue is insufficient, which ultimately leads to RPE cell damage (6). Studies have shown that the main mechanism of RPE cell damage is intracellular mitochondrial dysfunction (7). The RPE cells located in the outermost layer of the retina are susceptible to oxidative damage due to long-term exposure to light stimulation and hyperoxia, which produces chronic oxidative stress. Hyperglycemia further promotes the process of oxidative stress, thereby causing mitochondrial function damage, which ultimately leads to the impairment of cell function and activity (8). Therefore, how to effectively protect the internal mitochondrial function of RPE cells may be an effective means to treat DR lesions.

Genipin (GE) has been shown to be an effective treatment for retinal pigment epithelium injury through the development of diabetes drugs (9). Derived from the extraction and purification of gardenia jasminoides, GE has effective anti-inflammatory, antioxidant, and anti-diabetes properties (10). A previous study has shown that GE can effectively control blood glucose fluctuations in patients with type 2 diabetes (11). At the same time, a study has also shown that GE can effectively protect against RPE cell damage (12). However, there is no consensus on the molecular regulatory mechanism of GE in the protection of RPE cell function. By reviewing the literatures, a study has shown that the expression of Nrf2 signal axis, ERK signal axis and PI3K/AKT signal axis are all regulated by GE (13). As a ubiquitous intracellular regulatory pathway, AKT signaling pathway has been shown to be significantly overexpressed in retinal epithelial cells induced by high glucose. GE can significantly inhibit AKT signal pathway in retinal epithelial cells induced by high glucose (13).

In order to preliminarily predict the molecular mechanism of GE in the protection of RPE cells, bioinformatics analysis was conducted to identify the downstream proteins of differentially expressed genes located in the *AKT* pathway during GE treatment of RPE cells. The results showed that only RPRL and *JAK2* were downstream differential expression factors of *AKT*. RPRL, or prolactin, is closely related to breast diseases (14). *JAK2* is closely related to inflammatory responses and mitochondrial damage in the body (15). A previous study showed that *JAK2* was activated in RPE cells under hyperglycemia and the inflammatory response was aggravated (16). This finding suggests that the therapeutic effect of GE may be exerted by regulating the expression of *JAK2* through the *AKT* signaling pathway. But how does the *AKT* protein regulate JAK expression? This study suggests that the expression of *JAK2* may be further regulated by regulating the expression of microRNAs (miRNAs). In this study, the target miRNA of *JAK2* was predicted by the TargetScan, miRDB, and DIANA databases and the intersection was taken. The results showed that *miR-4429* has a targeted binding effect to *JAK2*, and a previous study has shown that *miR-4429* is a downstream regulatory molecule of *AKT* (17).

On this basis, the present study investigated whether GE could protect the retinal pigment epithelium from mitochondrial damage under hyperglycemic conditions through the *AKT* pathway mediated by the *miR-4429*/*JAK2* signaling axis. We present the following article in accordance with the ARRIVE reporting checklist (available at https://atm.amegroups.com/article/view/10.21037/atm-22-2219/rc).

Methods

Bioinformatics analysis

The Gene Expression Omnibus (GEO) database (https://

www.ncbi.nlm.nih.gov/geo/) was searched using the keywords ("RPE") AND ("GE") to obtain the dataset of diabetes patients and healthy subjects for comparative analysis by gene chip technology. Differential gene analysis was performed using the GEO online analysis tool GEO2R. P value <0.01 and |log fold change (FC)| >1 were used to screen differentially expressed genes. Downstream proteins of the *AKT* pathway were obtained with the Kyoto Encyclopedia of Genes and Genomes (KEGG) website. TargetScan (https://www.targetscan.org/vert_71/), miRDB (http://www.mirdb.org/cgi-bin/search.cgi), and DIANA (http://diana.imis.athena-innovation.gr/DianaTools/index.php) databases were further used to determine *JAK2*-targeted miRNAs. The study was conducted in accordance with the Declaration of Helsinki (as revised in 2013).

Reagents, antibodies, and kit sources

Dulbecco's modified Eagle medium (DMEM; Hyclone, Logan, UT, USA; SH30021.01B), fetal bovine serum (FBS; Hyclone; SH30396.03), phosphate-buffered saline (PBS) solution containing penicillin-streptomycin (STZ) (Hyclone; SH30256.01), Cell Counting Kit-8 (CCK-8) kit (Beijing, China; CA1210), enzyme-linked immunosorbent assay (ELISA) matrix metalloproteinases-2 (MMP-2) kit (Abnova, Taipei; E-KA0393), ELISA tumor necrosis factor-β (TNF-β) kit (Shenzhen, China; ZK-H063), Reverse Transcription System (Takara, Beijing, China; RR047A), and quantitative polymerase chain reaction (qPCR) kit (Takara; RR430B) were purchased for this study.

Cell culture, treatment, and grouping

The human RPE cell line ARPE-19 was selected for this study (Stem Cell Bank of Chinese Academy of Science, GNHu45). After obtaining the cells, the cells were inoculated in DMEM medium containing 10% FBS for culture. The cells were cultured in a 5% CO_2 incubator at 37 ℃. The cells were replaced with medium every day and the cell morphology was observed under an inverted microscope. Cell passaging was carried out when the cell density grew to about 90%.

CCK-8 assay

APRE-19 cells were treated according to different grouping treatment conditions and inoculated into 96-well plates, then incubated in a constant temperature incubator. The CCK-8 kit was used to detect cell proliferation at 72 hours after inoculation. The 96-well plates were taken out of the constant temperature incubator, the medium was discarded from each well, 100 μL CCK-8 solution was added to each well, and plates were placed in the incubator for 2 hours. Finally, the absorbance of each well was measured at 450 nm.

Establishment of lentivirus knockdown/overexpression cell lines

MiR-4429-mimics and si-mimics lentiviruses were obtained from GeneChem (https://www.genechem.com.cn/index/index/index.html). The virus was constructed, sequenced, produced, titered, and transported to the laboratory in cold chain packaging. The ARPE-19 cell line was used as the research object. When the cell growth density reached 90%, the cells were digested by trypsin and suspended again. The obtained cells were inoculated in a 6-well plate at a density of 1×10^5/well and incubated in a 37 ℃ incubator for 24 hours until they adhered to the wall. The purchased lentivirus was diluted with DMEM solution containing 10% FBS at a ratio of 1:10. After the medium in the 6-well plate was discarded, 1 ml diluent containing lentivirus was added to each well. After 24 hours of culture in a 37 ℃ incubator, the culture medium containing lentivirus was discarded, then 2 mL DMEM medium containing 10% FBS was added, and the culture was continued in the incubator.

Dual luciferase reporter assay

Starbase 2.0 was used to predict the binding site of *miR-4429* to *JAK2* and select the appropriate mutation site. Construction of the dual luciferase reporter gene of *JAK2* contained the *miR-4429* prediction site. *MiR-4429*-wild type (WT) + mimic control, *miR-4429*-WT + *JAK2* mimic, *miR-4429*-WT + inhibitor control, *miR-4429*-WT + *JAK2* inhibitor, *miR-4429*-mutant (MUT) + mimic control, *miR-4429*-MUT + *JAK2* mimic, *miR-4429*-MUT + inhibitor control, and *miR-4429*-MUT + *JAK2* inhibitor were used to transfect ARPE-19 cells after high glucose induction. At 48 hours after successful transfection, luciferase activity was measured using a dual luciferase reporter assay system (Promega, Madison, WI, USA).

Reverse transcription-PCR (RT-PCR) assay

ARPE-19 cells in different groups were treated according to different treatment conditions, and the cells were digested

Table 1 The primer sequences used in the RT-PCR assay

Gene name	Primer sequence
CYT C1	
Forward	5'-GGTGGAAAAGGCGGGAAAC-3'
Reverse	5'-CCGTGTAAGAAAATCCTGGTGC-3'
AKT	
Forward	5'-CAGGTGCGGACAT TCTAC-3'
Reverse	5'-TTGCGTTCTTAGGCTTCTC-3'
MiR-4429	
Forward	5'-CCTGAAAAGCTGGGCTGAGAG-3'
Reverse	5'-GCATAGACCTGAATGGCGGTA-3'
JAK2	
Forward	5'-TCTGTGGGAGATCTGCAGTG-3'
Reverse	5'-TTTCAGAGCTGTCATCCGTG-3'
β-actin	
Forward	5'-GCCCTGAGGCTCTCTTCCA-3'
Reverse	5'-GCGGATGTCGACGTCACA-3'

RT-PCR, reverse transcription-polymerase chain reaction.

by trypsin, centrifuged, and collected 72 hours after treatment (15). Total RNA was extracted by the TRIzol method. The concentration and purity of RNA in 2 μL solution were determined by a microspectrophotometer. The reverse transcription reaction system was established using the Takara reverse transcription kit to reverse transcribe RNA into complementary DNA (cDNA). Using the qPCR kit to establish the cDNA reaction system, the conditions were as follows: 95 ℃ 10 min, 95 ℃ 30 sec, 60 ℃ 30 sec, 40 cycles. The dissolution curve was analyzed, and the expression levels of *CYT C1*, *AKT*, *miR-4429*, and *JAK2* in each sample were statistically analyzed by the $2^{-\Delta\Delta CT}$ method. Primers of each gene are shown in *Table 1*.

Western blot (WB)

ARPE-19 cells were treated according to different grouping conditions, and the cells were trypsin digested, centrifuged, and collected 120 hours after treatment. Cell contents were obtained by lysing cells, and total proteins in cells were collected by centrifugation. The protein concentration was detected by the BCA method. After the protein concentration was quantified, SDS-PAGE electrophoresis was performed for each group of tissue/cells. After electrophoresis, the proteins separated by electrophoresis were transferred to PVDF membranes using a transfer device. The PVDF membrane was then removed and sealed with 5% skim milk for 1 hour, then rinsed with PBS. Subsequently, primary anti-*AKT* (1:500), *CYT C1* (1:500), and *JAK2* (1:500) were added and incubated overnight. The secondary antibody (sheep anti-rabbit antibody, 1:1,000) was added and incubated for 1 hour. Finally, the PVDF membrane signals were detected by the chemiluminescence imaging system.

Seahorse cellular energy metabolism analysis

First, each group of cells was inoculated into a Seahorse Xfe microplate, and the Seahorse Xfe24 cell energy metabolism analyzer was turned on for preheating the day before the experiment. At the same time, 1 mL calibration solution was added to the hydration plate in the analyzer and placed in a constant temperature cell incubator overnight. On the day of the experiment, 1.2 mL 1.0 M glucose solution, 1.2 mL 100 mM pyruvate solution, and 1.2 mL glutamine solution were added into 120 mL DMEM medium. According to the instructions, 630, 720, and 540 μL detection solutions were added to oligase, FCCP, and rotenone/antimycin reagent tubes, respectively. Cells in each group were removed from the incubator, and 500 μL detection solution was added to each well to clean cells. The optimal concentration of FCCP was obtained by FCCP titration. Then, the hydration plate and the probe plate that had been dosed were placed in the instrument and the grouping and procedure for the experiment were set up. After data acquisition, the obtained results were input into Wave software for data processing, and the results were analyzed in combination with Seahorse experimental data.

Animal feeding and grouping

A total of 45 6-week-old C57BL/6 mice (18±20 g, purchased from Nanjing Junjunke Biological Engineering Co., Ltd., Nanjing, China) were used as the research objects. The mice were raised in a specific pathogen free (SPF) environment. Animal experiments were performed under a project license (No. QMU-AECC-2021-244) granted by Animal Ethical Committee of Qiqihar Medical University, in compliance with national guidelines for the care and use of animals. The operation and treatment procedures were in accordance with the relevant regulations of the Experimental Animal Ethics Committee of Qiqihar

Medical University. A protocol was prepared before the study without registration. Before the experiment, mice were fed with a standard mice diet for 1 week. The breeding environment included room temperature 2–25 ℃, relative humidity 55%±5%, and light/darkness cycle for 12 hours. The mice were randomly divided into three groups: control group, diabetic model group, and diabetic + GE group, with 15 mice in each group.

Preparation of the diabetic mouse model: after 1 week of adaptive feeding, the mice were fed with a high-fat diet for 4 weeks. At the end of the fifth week, STZ (60 mg/kg) was injected intraperitoneally for 3 days to induce type 2 diabetes. At 72 hours after induction, blood samples were collected from the tail vein, and fasting blood glucose of the mice was measured. Fasting blood glucose was more than 11.1 mmol/L, indicating that the modeling was successful.

GE treatment: after successful establishment of the diabetic mouse model, mice in the diabetic model + GE group were given GE (25 mg/kg) intragastric therapy once a day for 1 week.

Electroretinogram (ERG)

ERG detection is mainly divided into EGR detection under dark adaptation and ERG detection under light stimulation. The dark adaptation test was performed by injecting 50 mg/kg pentobarbital sodium intraperitoneally and dilating pupils with compound tropicamide drops after overnight exposure to a dark environment. After anesthesia, the mice were fixed in the prone position on the test table, and the annular electrodes were placed in front of both eyes and contacted with the cornea. Connect the electrode correctly and light response stimulation were performed. In the process of light stimulus detection, white light flashing stimuli were provided for 6 times. The intensity was 0.65 log CD·s/m, each intensity was attenuated 1 log by the neutral filter, the single light duration was 10 μs, and the stimulation interval was 12 s. Double channel synchronous sampling recording was performed, with frequency 1–1,000 Hz and amplification 10,000 times. The measurement was repeated for each light intensity at least 3 times.

Statistical analysis

SPSS 23.0 statistical software was used for analysis. The obtained data were expressed in the form of mean ± standard deviation (SD). Analysis of variance was used for comparisons between multiple groups. The independent sample *t*-test between two groups was performed for indicators with statistically significant results of analysis of variance. P<0.05 was considered statistically significant.

Results

GE protects the mitochondrial function of RPE cells under hyperglycemia

The CCK-8 assay showed that the activity of RPE cells was significantly decreased under hyperglycemia (P<0.05), but increased after adding GE (P<0.05; *Figure 1A*). RT-PCR results showed that the expression of *CYT C1* in RPE cells under hyperglycemia was significantly increased (P<0.05), and the expression of *CYT C1* in RPE cells was significantly decreased after adding GE (P<0.05; *Figure 1B*). The comparison of energy metabolism analysis results showed that the basal respiration rate, maximum respiration capacity, and adenosine triphosphate (ATP) synthesis capacity were significantly decreased under hyperglycemia (P<0.05), and all significantly increased after adding GE (P<0.05). Energy metabolism analysis showed that mitochondrial permeability increased in RPE cells under hyperglycemia (P<0.05), and decreased significantly after adding GE (P<0.05; *Figure 1C-1G*).

WB results showed that the expression of *CYT C1* was significantly increased under hyperglycemia (P<0.05), and decreased significantly after adding GE (P<0.05; *Figure 2A,2B*). The expression of *AKT* in RPE cells was significantly increased after adding GE (*Figure 2C*).

GE regulates mitochondrial damage in hyperglycemia through the AKT signaling pathway

This study further clarified the specific mechanism of GE in protecting RPE cells against mitochondrial damage under hyperglycemia by adding an *AKT* pathway inhibitor in the environment of GE. CCK-8 assay results showed that RPE cell activity decreased under hyperglycemia, and increased after adding GE. After adding GE and *AKT* inhibitors, the cell activity decreased significantly (P<0.05; *Figure 3A*). RT-PCR results showed that the expression of *CYT C1* increased in RPE cells under hyperglycemia, decreased significantly after adding GE, and increased significantly after adding GE and *AKT* inhibitor (P<0.05; *Figure 3B*). The results of energy metabolism analysis showed that the basal respiration rate, maximum respiration capacity,

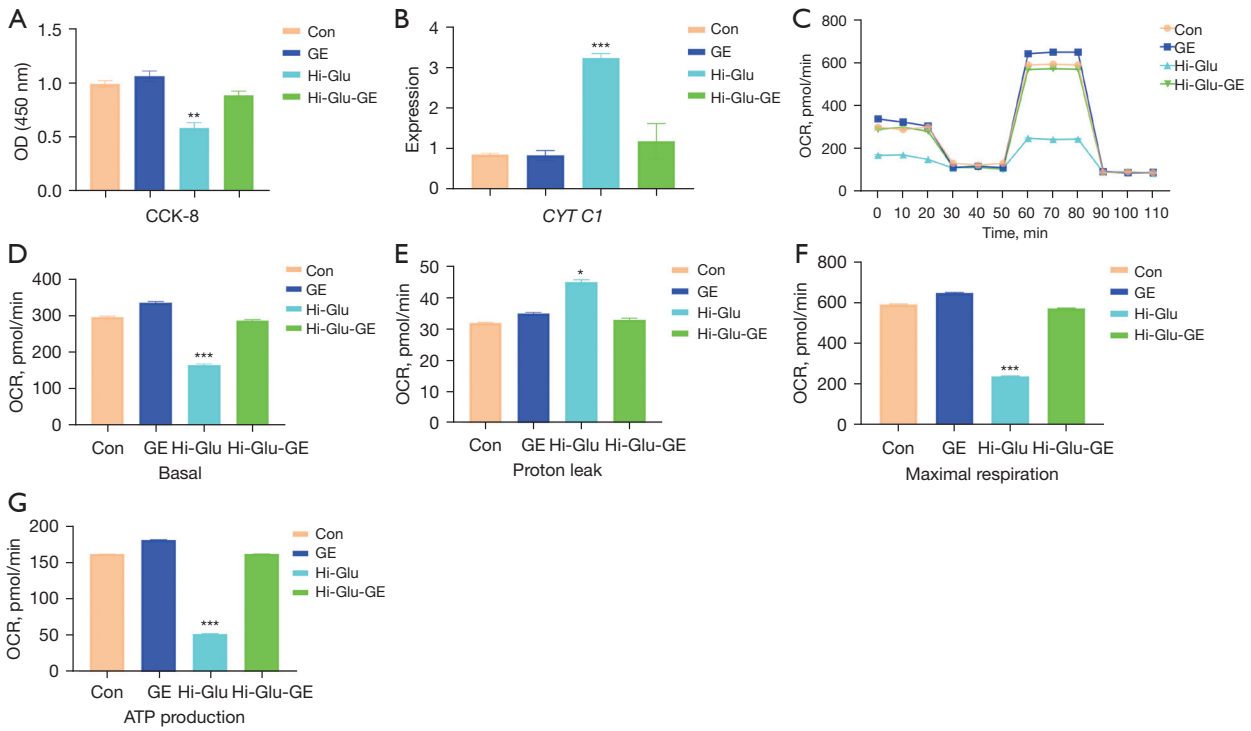

Figure 1 GE protects mitochondrial function in RPE cells induced by high glucose. (A) The CCK-8 assay was used to detect the changes in cell activity after high glucose combined with GE treatment under hyperglycemia; (B) RT-PCR was used to detect the changes in *CYT C1* expression after high glucose combined with GE treatment under hyperglycemia; (C) the results of Seahorse cell energy metabolism analysis; (D-G) energy metabolism analysis results showed the changes in the basal respiration rate, maximum respiratory capacity, and ATP synthesis capacity after high glucose combined with GE treatment under hyperglycemia (***P<0.01, **P<0.05, *P<0.1). OD, optical density; GE, genipin; CCK-8, Cell Counting Kit-8; OCR, O_2 consumption rate; ATP, adenosine triphosphate; RPE, retinal pigment epithelial; RT-PCR, reverse transcription-polymerase chain reaction.

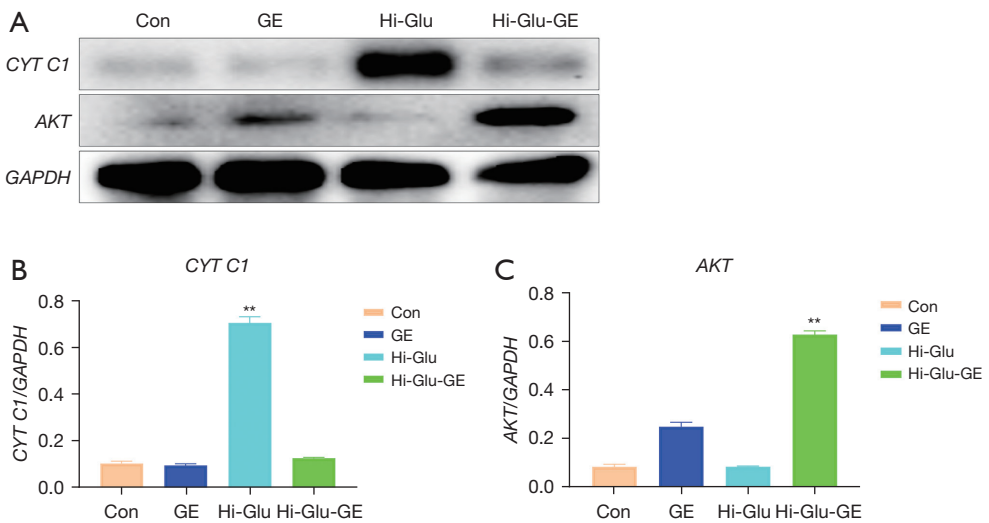

Figure 2 Changes in the expression of *CYT C1* and *AKT* in RPE cells under GE treatment and hyperglycemia. (A) WB was used to detect *CYT C1* and *AKT* expression in cells of each group; (B,C) WB was used to detect the expression changes of *CYT C1* and *AKT* in each group after high glucose combined with GE treatment under hyperglycemia (**P<0.05). GE, genipin; RPE, retinal pigment epithelial; WB, western blot.

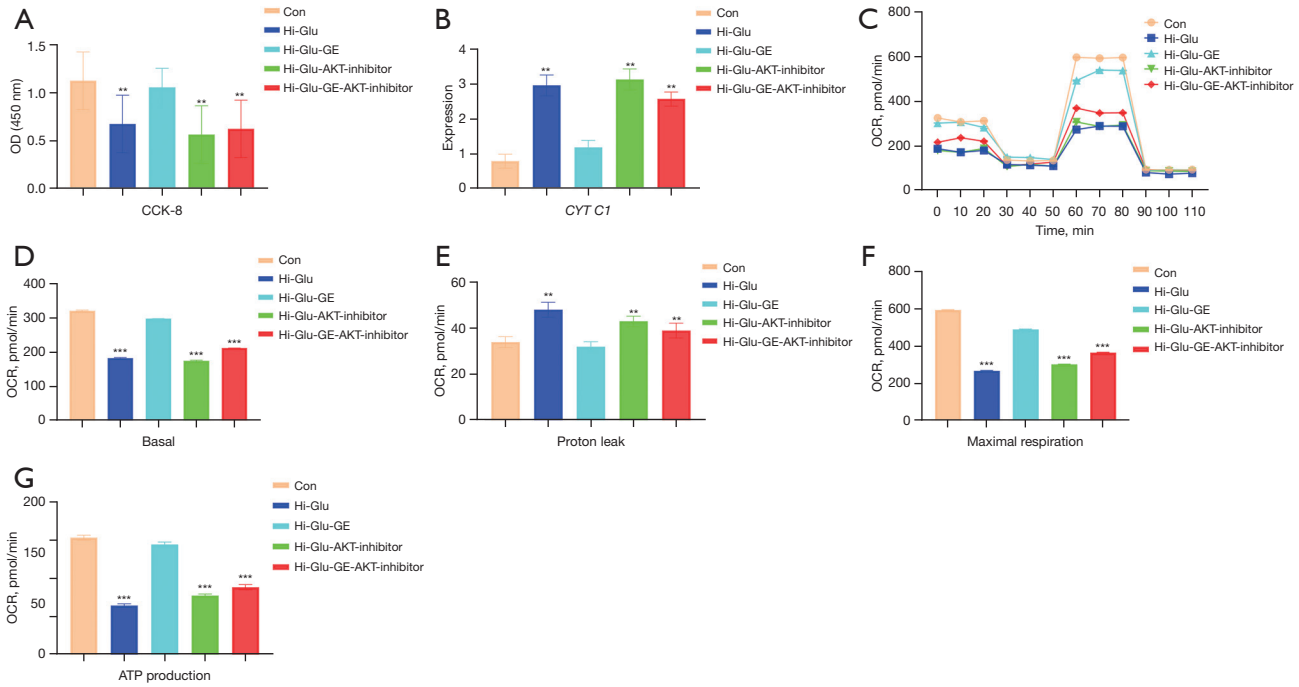

Figure 3 GE protects mitochondrial function in RPE cells under hyperglycemia through the *AKT* signaling pathway. (A) The CCK-8 assay was used to detect the changes in RPE cell activity after adding GE, *AKT* inhibitor, and GE combined with *AKT* inhibitor under hyperglycemia; (B) RT-PCR was used to detect the changes of *CYT C1* expression in RPE cells after adding GE, *AKT* inhibitor, and GE combined with *AKT* inhibitor under hyperglycemia; (C) the results of Seahorse cell energy metabolism analysis; (D-G) energy metabolism analysis results showed the changes in the basal respiration rate and maximum respiration after adding GE, *AKT* inhibitor, and GE combined with *AKT* inhibitor under hyperglycemia capacity, ATP synthesis capacity (***P<0.01, **P<0.05). OD, optical density; GE, genipin; CCK-8, Cell Counting Kit-8; OCR, O_2 consumption rate; ATP, adenosine triphosphate; RPE, retinal pigment epithelial; RT-PCR, reverse transcription-polymerase chain reaction.

and ATP synthesis ability decreased significantly under hyperglycemia (P<0.05), though increased significantly after adding GE, and decreased significantly after adding GE and *AKT* inhibitors (P<0.05). Mitochondrial permeability increased in RPE cells under hyperglycemia (P<0.05), decreased significantly after adding GE (P<0.05), and increased significantly after adding GE and *AKT* inhibitor (P<0.05; *Figure 3C-3G*).

WB results showed that the expression of *CYT C1* was increased in RPE cells under hyperglycemia, and decreased significantly after adding GE, while the expression of *CYT C1* was significantly increased after adding GE and *AKT* inhibitor (P<0.05; *Figure 4A,4B*). The expression of *AKT* in RPE cells increased significantly after adding GE (P<0.05), and decreased significantly after adding GE and *AKT* inhibitor (P<0.05; *Figure 4C*).

GE regulates the mitochondrial damage of RPE cells under hyperglycemia by mediating JAK2 through the AKT pathway

To further clarify the downstream molecules regulated by GE through *AKT*, we obtained the GSE35934 dataset from the GEO database through bioinformatics analysis. It was mainly used to analyze the mRNA expression changes during GE treatment, and GEO2R was used to obtain differentially expressed genes (*Figure 5A,5B*). Finally, 76 significantly differentially expressed genes were obtained by setting the threshold. Meanwhile, 326 genes related to the KEGG-*AKT* pathway were obtained through KEGG analysis. By taking the intersection of Venn diagrams, we obtained 2 differentially expressed downstream proteins of *AKT*, namely RPRL and *JAK2* (*Figure 5C,5D*). RPRL is

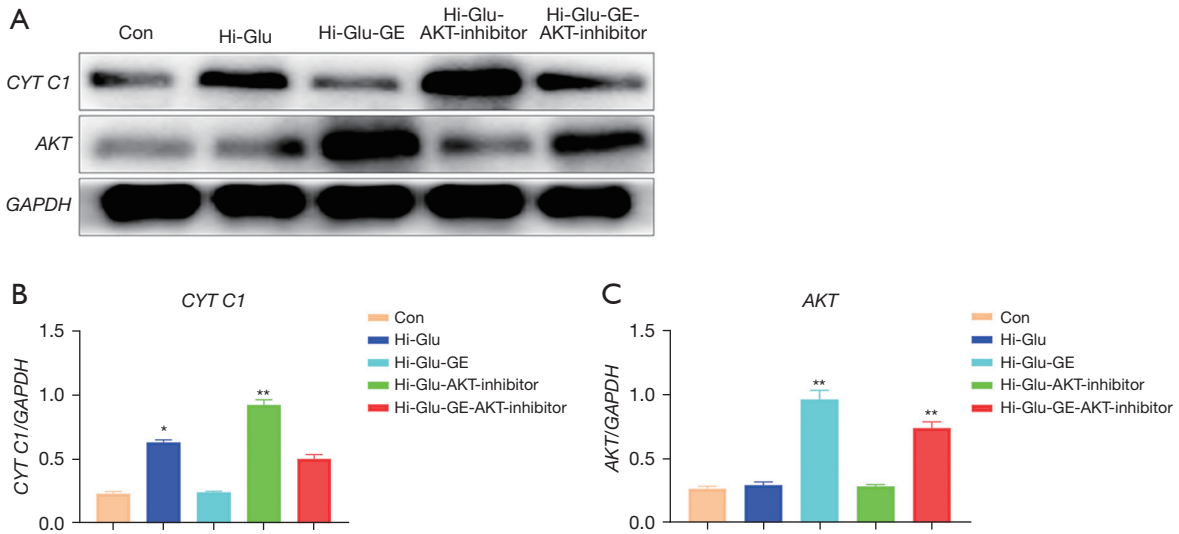

Figure 4 GE regulates the expression changes of *CYT C1*, *AKT* and *JAK2* in RPE cells under hyperglycemia through *AKT*. (A) WB was used to detect *CYT C1* and *AKT* expression in cells of each group; (B,C) WB was used to detect the expression changes of *CYT C1* and *AKT* in each group after adding GE and *AKT* inhibitor under hyperglycemia (**P<0.05, *P<0.1). GE, genipin; RPE, retinal pigment epithelial; WB, western blot.

mainly related to breast diseases, while *JAK2* is related to cell activities such as apoptosis. Therefore, in this study, *JAK2* was considered to be a downstream molecule of *AKT* after GE treatment of high glucose-induced RPE cell damage.

CCK-8 assay results showed that the cell activity was significantly decreased after adding GE and *AKT* inhibitor (P<0.05). There was no significant decrease in cell activity after adding GE and *JAK2* inhibitor. The cell activity was still higher after adding GE combined with *AKT* inhibitor and *JAK2* inhibitor (P<0.05; *Figure 6A*). RT-PCR results showed that the expression of *CYT C1* was significantly decreased after adding GE, though increased after adding GE and *AKT* inhibitors (P<0.05), and the expression of *CYT C1* was significantly decreased compared with that under hyperglycemia after adding GE and *JAK2* inhibitor (P<0.05). The expression of *CYT C1* was significantly decreased compared with that under hyperglycemia after adding GE combined with *AKT* inhibitor and *JAK2* inhibitor (P<0.05; *Figure 6B*). The results of energy metabolism analysis showed that the basal respiration rate, maximum respiration capacity, and ATP synthesis capacity of RPE cells were significantly increased after adding GE, and decreased significantly after adding GE and *AKT* inhibitor (P<0.05). The basal respiration rate, maximum respiration capacity, and ATP synthesis capacity of RPE cells were significantly decreased compared with that under hyperglycemia after adding GE and *JAK2* inhibitor (P<0.05), and the same result was also obtained after adding GE combined with *AKT* inhibitor and *JAK2* inhibitor (P<0.05). Mitochondrial permeability was significantly decreased after adding GE (P<0.05), while mitochondrial permeability was significantly increased after adding GE and *AKT* inhibitor (P<0.05). Mitochondrial permeability was significantly decreased after adding GE and *JAK2* inhibitor (P<0.05), and mitochondrial permeability was also significantly decreased (P<0.05) after adding GE combined with *AKT* inhibitor and *JAK2* inhibitor (*Figure 6C-6G*).

WB results showed that the expression of *CYT C1* was significantly decreased after adding GE compared with that under hyperglycemia. The expression of *CYT C1* was significantly increased after adding GE and *AKT* inhibitor, decreased after adding GE and *JAK2* inhibitor, and decreased after adding GE combined with *AKT* inhibitor and *JAK2* inhibitor (P<0.05; *Figure 7A*,*7B*). The expression of *AKT* in RPE cells was significantly increased after adding GE (P<0.05), and decreased after adding GE and *AKT* inhibitor (P<0.05). The expression of *AKT* was not significantly different from the GE group after adding *JAK2* inhibitor, but the expression of *AKT* decreased significantly after adding GE combined with *AKT* inhibitor and *JAK2* inhibitor (P<0.05; *Figure 7C*). The expression of *JAK2* was significantly decreased compared with that under hyperglycemia after

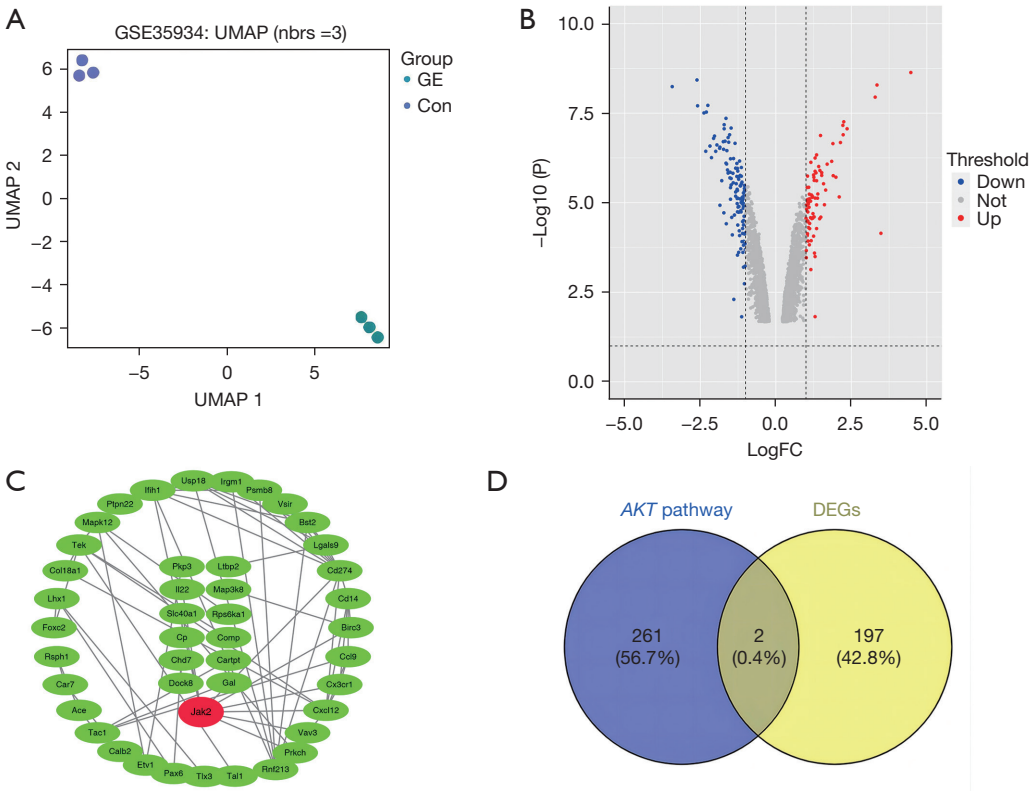

Figure 5 Bioinformatics analysis predicts the mechanism by which GE protects against RPE mitochondrial damage under hyperglycemia. (A) A cluster diagram was used to evaluate the expression changes of intracellular molecules after adding GE under hyperglycemia; (B) a volcano plot was used to display differentially expressed genes; (C) PPI network was used to select core targets in differentially expressed genes; (D) a Venn diagram was used to identify the shared genes of differentially expressed genes and *AKT* pathway-related genes. UMAP, Uniform Manifold Approximation and Projection; GE, genipin; FC, fold change; DEGs, differentially expressed genes; RPE, retinal pigment epithelial; PPI, protein-protein interaction.

adding GE, and increased significantly after adding GE and *AKT* inhibitor. The expression of *JAK2* was significantly decreased after adding GE and *JAK2* inhibitor, and also decreased (P<0.05) after adding GE combined with *AKT* inhibitor and *JAK2* inhibitor (*Figure 7D*).

GE protects against the mitochondrial damage of RPE cells under hyperglycemia by mediating miR-4429/JAK2 through the AKT pathway

In order to further clarify the specific mechanism of GE-mediated *AKT* in the protection of RPE mitochondrial function under hyperglycemia by inhibiting *JAK2*, this study predicted *JAK2*-targeted miRNAs using TargetScan 7.2, MIRDB, and Starbase 3.0 and obtained the intersection. Finally, 25 miRNAs were obtained (*Figure 8A*). Based on the literature review, *miR-4429* was shown to be a downstream miRNA molecule of *AKT*. The potential binding site of *miR-4429* and *JAK2* was predicted by online databases (*Figure 8B*). Therefore, this study suggested that GE protects against the mitochondrial damage of RPE cells under hyperglycemia by mediating *miR-4429/JAK2* through the *AKT* pathway.

In this study, the corresponding hypothesis was verified by constructing *miR-4429*-mimics and si-*miR-4429* lentiviral vectors and combining inhibited or activated with *AKT* and *JAK2* signaling. CCK-8 assay results showed that compared with adding GE under hyperglycemia, the cell activity was significantly inhibited after adding *AKT* inhibitor, increased after adding *miR-4429*-mimics, and inhibited after adding si-*miR-4429* (P<0.05; *Figure 9A*). RT-PCR showed that the expression of *CYT C1* was significantly increased after adding *AKT* inhibitor, decreased after adding *miR-4429*-mimics, and increased after adding si-*miR-4429*

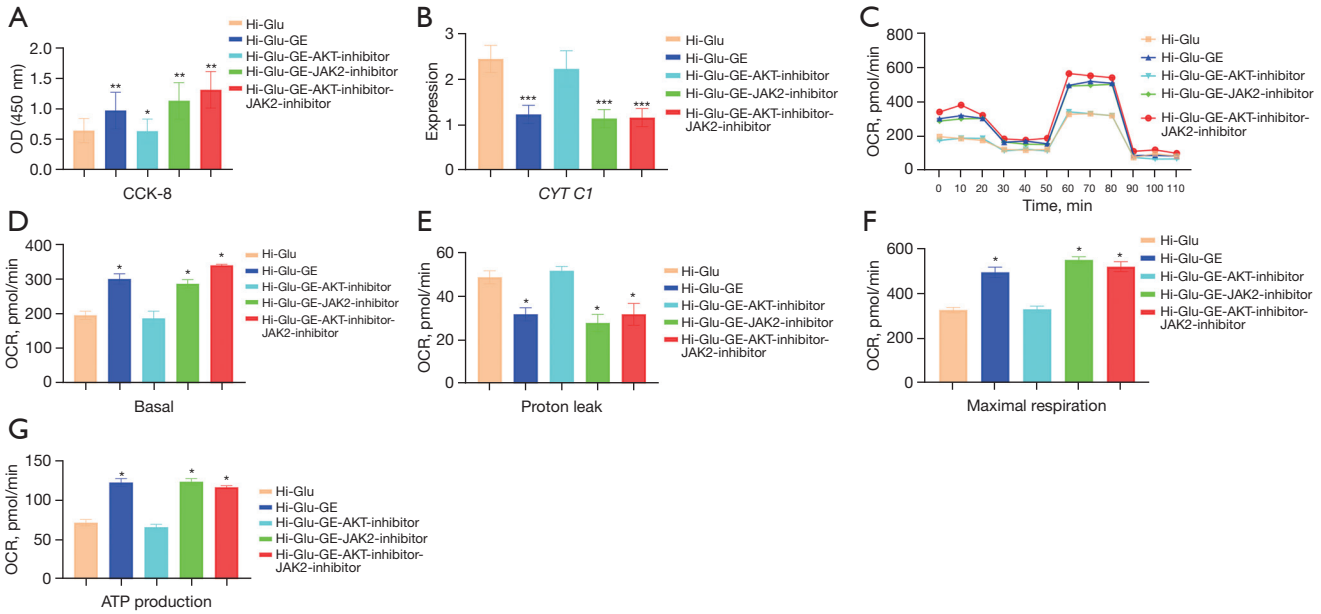

Figure 6 GE protects mitochondrial function in RPE cells under hyperglycemia via *AKT/JAK2*. (A) The CCK-8 assay was used to detect the changes in RPE cell activity after adding GE, *AKT* inhibitor, *JAK2* inhibitor, and GE combined with *AKT* inhibitor and *JAK2* inhibitor under hyperglycemia; (B) RT-PCR was used to detect the expression changes of *CYT C1* in RPE cells after adding GE, *AKT* inhibitor, *JAK2* inhibitor, and GE combined with *AKT* inhibitor and *JAK2* inhibitor under hyperglycemia; (C) the results of Seahorse cell energy metabolism analysis; (D-G) energy metabolism analysis results showed the changes in the basal respiratory rate, maximal respiratory capacity, and ATP synthesis capacity after adding GE, *AKT* inhibitor, and GE combined with *AKT* inhibitor under hyperglycemia (***P<0.01, **P<0.05, *P<0.1). OD, optical density; GE, genipin; CCK-8, Cell Counting Kit-8; OCR, O_2 consumption rate; ATP, adenosine triphosphate; RPE, retinal pigment epithelial; RT-PCR, reverse transcription-polymerase chain reaction.

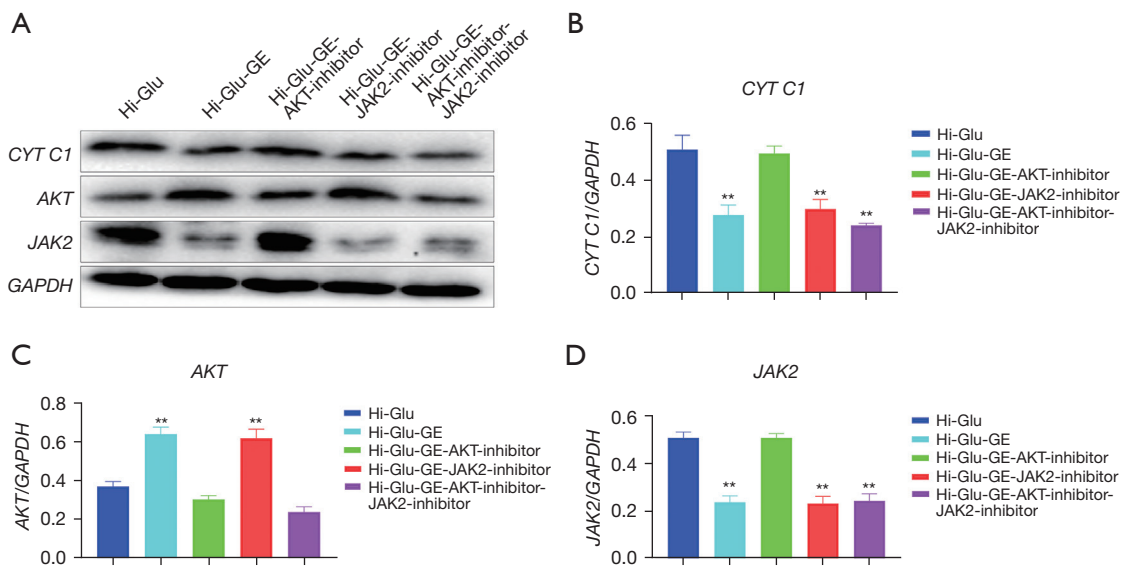

Figure 7 GE regulates the changes in the expression of *CYT C1*, *AKT* and *JAK2* in RPE cells under hyperglycemia through *AKT/JAK2*. (A) WB was used to detect *CYT C1*, *AKT* and *JAK2* expression in each group; (B-D) WB was used to detect the expression changes of *CYT C1* and *AKT* in each group after adding GE, *AKT* inhibitor, *JAK2* inhibitor, and GE combined with *AKT* inhibitor and *JAK2* inhibitor under hyperglycemia (**P<0.05). GE, genipin; RPE, retinal pigment epithelial; WB, western blot.

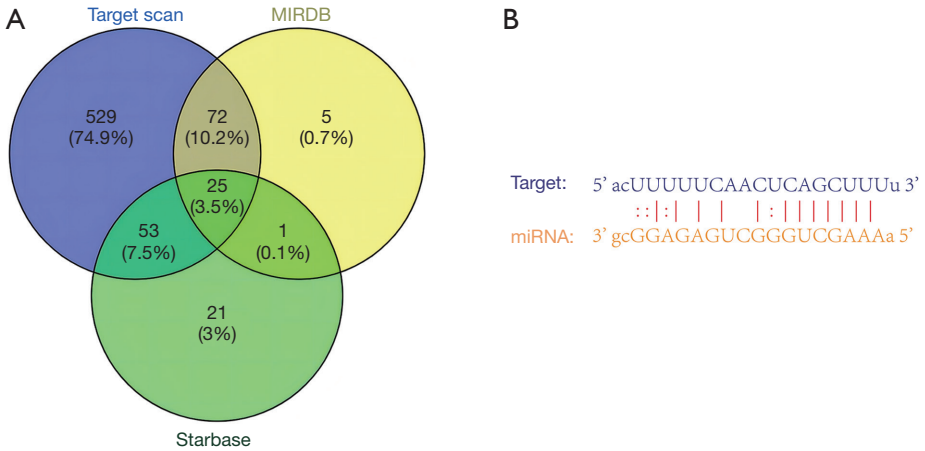

Figure 8 Bioinformatics analysis identifies miRNAs that have a targeted regulatory relationship with *JAK2*. (A) Targetscan 7.2, miRDB, and Starbase 3.0 were used to predict miRNAs that have a targeting relationship with *JAK2*; (B) the targeted binding site of *JAK2* to *miR-4429*. MiRNA, microRNA.

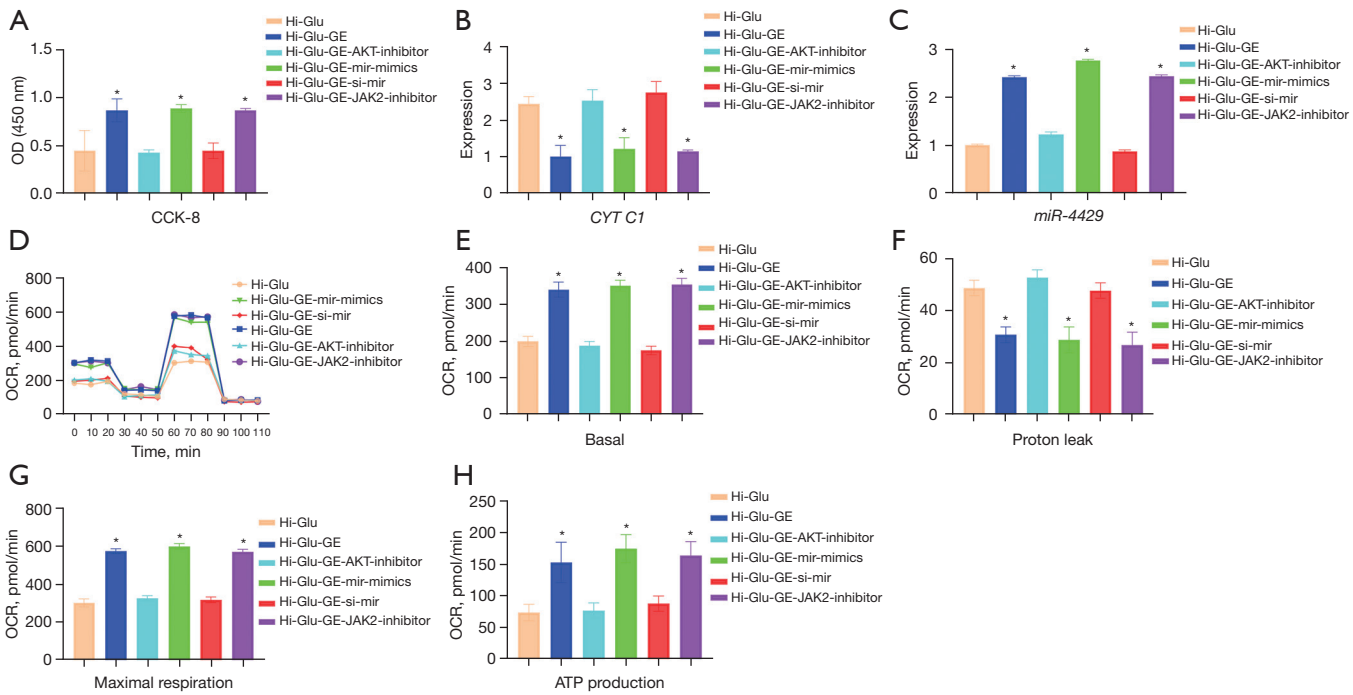

Figure 9 GE protects mitochondrial function in RPE cells under hyperglycemia through *AKT*/*miR-4429*/*JAK2*. (A) The CCK-8 assay was used to detect the changes in RPE cell activity after adding GE, GE combined with *AKT* inhibitor, and GE combined with *miR-4429*-mimics, si-*miR-4429*, and *JAK2* inhibitor under hyperglycemia; (B) RT-PCR was used to detect the expression changes of *CYT C1* in RPE cells after adding GE, GE combined with *AKT* inhibitor, and GE combined with *miR-4429*-mimics, si-*miR-4429*, and *JAK2* inhibitor under hyperglycemia; (C) RT-PCR was used to detect the expression changes of *miR-4429* in RPE cells after adding GE, GE combined *AKT* inhibitor, and GE combined with *miR-4429*-mimics, si-*miR-4429*, and *JAK2* inhibitor under hyperglycemia; (D) the results of Seahorse cell energy metabolism analysis; (E-H) energy metabolism analysis results showed the changes in the basal respiratory rate, maximal respiratory capacity, and ATP synthesis capacity after adding GE, GE combined with *AKT* inhibitor, and GE combined with *miR-4429*-mimics, si-*miR-4429*, and *JAK2* inhibitor (*P<0.1). OD, optical density; GE, genipin; mir, miR-4429; CCK-8, Cell Counting Kit-8; OCR, O_2 consumption rate; ATP, adenosine triphosphate; RPE, retinal pigment epithelial; RT-PCR, reverse transcription-polymerase chain reaction.

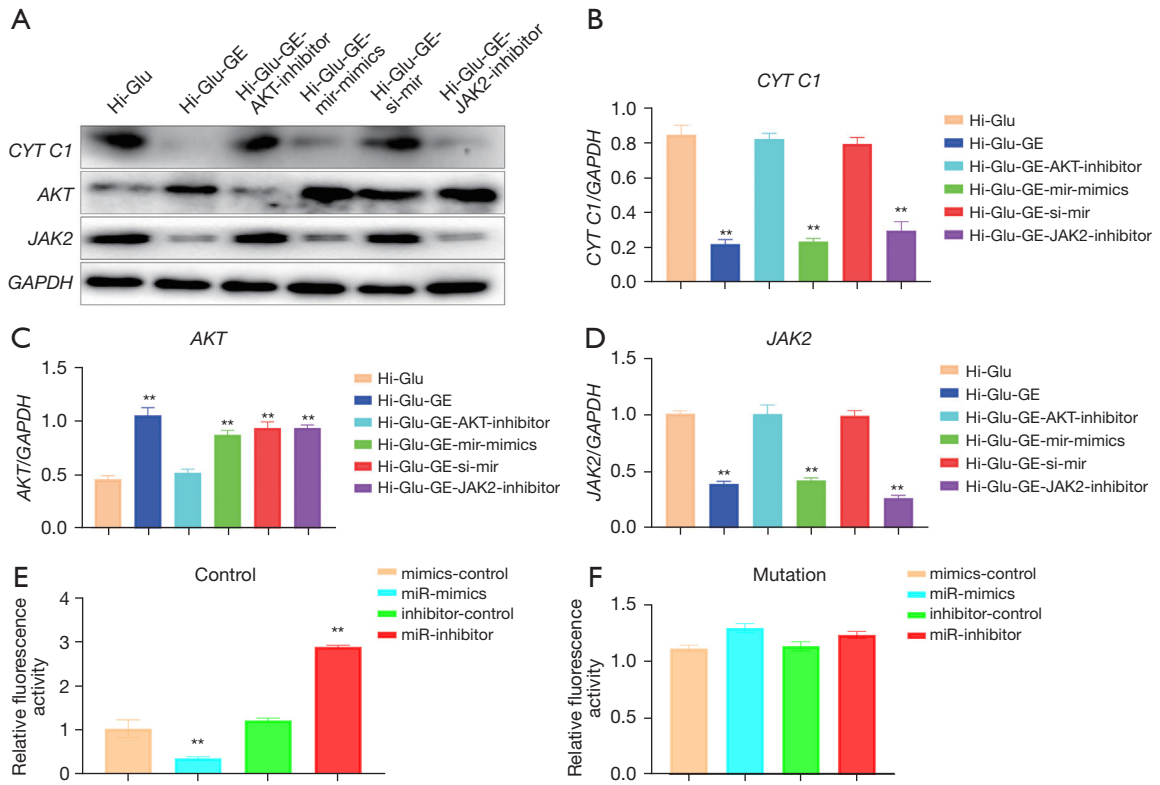

Figure 10 GE regulates the expression of *CYT C1*, *AKT* and *JAK2* changes in RPE cells under hyperglycemia through *AKT/miR-4429/JAK2*. (A) WB was used to detect the expression of *CYT C1*, *AKT* and *JAK2* in each group; (B-D) WB was used to detect the expression changes of *CYT C1* and *AKT* after adding GE, GE combined with *AKT* inhibitor, and GE combined with *miR-4429*-mimics, si-*miR-4429*, and *JAK2* inhibitor in each group (**P<0.05); (E,F) dual luciferase gene reporter assay confirmed that *miR-4429* targeted *JAK2* binding. GE, genipin; mir, miR-4429; RPE, retinal pigment epithelial; WB, western blot.

(P<0.05; *Figure 9B*). RT-PCR showed that the expression of *miR-4429* was significantly increased after adding GE, and inhibited after adding *AKT* inhibitor (P<0.05; *Figure 9C*). The results of energy metabolism analysis showed that the basal respiration rate, maximum respiration capacity, and ATP synthesis capacity were significantly decreased after adding *AKT* inhibitor (P<0.05), increased after adding *miR-4429*-mimics, and decreased after adding si-*miR-4429* (P<0.05). Mitochondrial permeability was significantly increased after adding *AKT* inhibitor, decreased after adding *miR-4429*-mimics, and increased after adding si-*miR-4429* (P<0.05; *Figure 9D-9H*).

WB was used to detect the expression of *CYT C1*, *AKT*, and *JAK2* (*Figure 10A*). The expression of *CYT C1* was significantly increased after adding *AKT* inhibitor, decreased after adding *miR-4429*-mimics, and increased after adding si-*miR-4429* (P<0.05; *Figure 10B*). The expression of *AKT* was significantly decreased after adding *AKT* inhibitor (P<0.05). After adding *miR-4429*-mimics, si-*miR-4429*, and *JAK2* inhibitor, the expression of *AKT* was significantly increased compared with adding *AKT* inhibitor (P<0.05). Meanwhile, there was no statistical difference in the GE group under hyperglycemia (P>0.05; *Figure 10C*). The expression of *JAK2* was significantly increased after adding *AKT* inhibitor, decreased after adding *miR-4429*-mimics, and increased after adding si-*miR-4429* (P<0.05; *Figure 10D*). The potential binding site of *miR-4429* and *JAK2* was predicted by online databases, and the dual luciferase gene reporter assay confirmed that *miR-4429* targeted *JAK2* binding (*Figure 10E,10F*).

Animal experiments verified the specific molecular mechanism of GE in the protection of RPE cells in diabetic mice

The results of ERG showed the intensity and amplitude

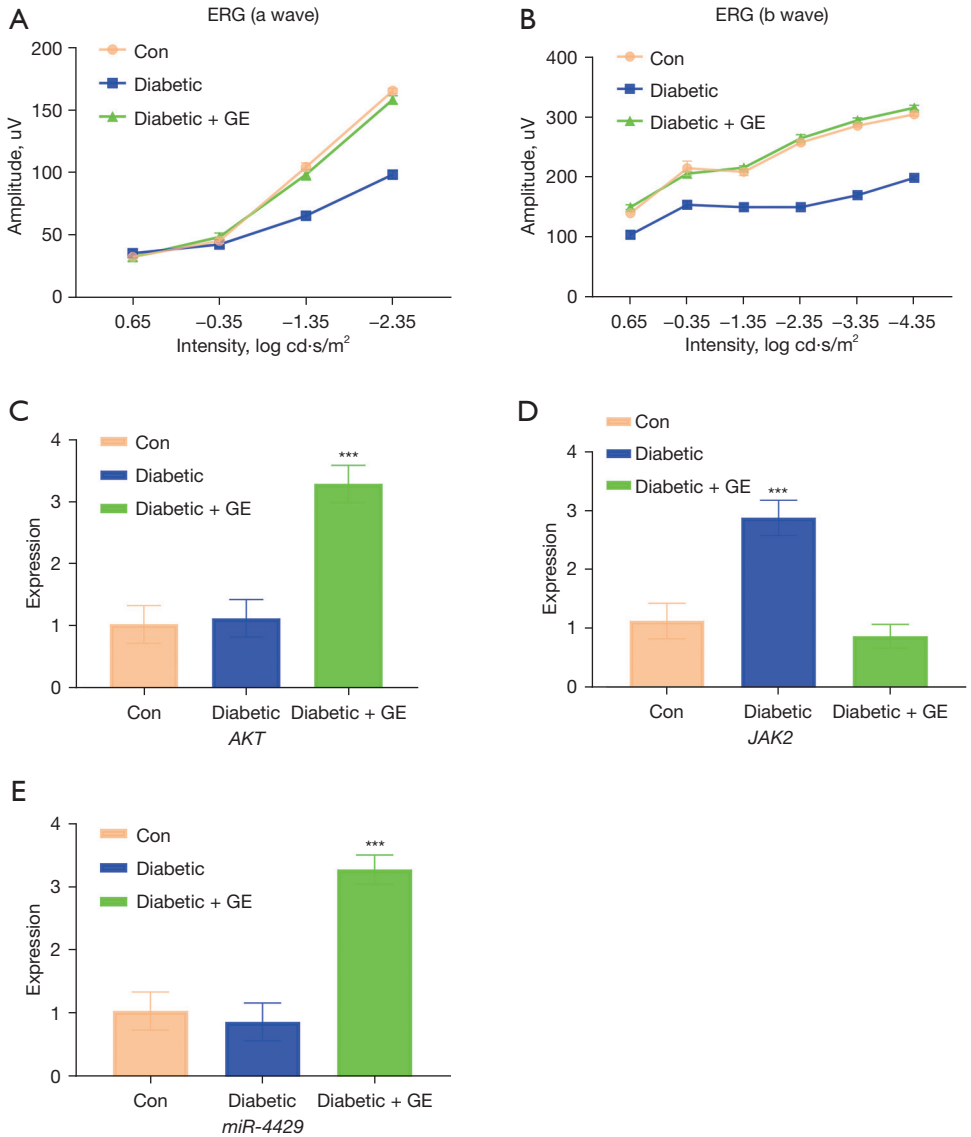

Figure 11 The effect of GE on RPE cells in diabetic mice. (A,B) ERG was used to detect the changes of a-wave and b-wave light intensity-amplitude in control diabetic mice and diabetic mice after GE treatment; (C-E) RT-PCR was used to detect the expression changes of *AKT*, *miR-4429*, and *JAK2* in RPE cells of control diabetic mice and diabetic mice after GE treatment (***P<0.01). ERG, electroretinogram; GE, genipin; RPE, retinal pigment epithelial; RT-PCR, reverse transcription-polymerase chain reaction.

of ERG wave A and wave B in each group. The results showed that the amplitudes of A and B waves in diabetic mice decreased significantly (P<0.05), while the amplitudes of A and B waves in diabetic mice increased significantly after adding GE (P<0.05; *Figure 11A,11B*). RT-PCR results showed that after adding GE, the expression of *AKT* and *miR-4429* in RPE cells was significantly increased (P<0.05), while the expression of *JAK2* was significantly decreased (P<0.05; *Figure 11C-11E*).

Discussion

In this study, bioinformatics analysis predicted that GE may protect RPE cells from damage by high glucose through *AKT/miR-4429/JAK2*. CCK-8 experiments showed that GE could regulate the *miR-4429/JAK2* signaling axis through the *AKT* pathway to protect RPE cell activity under hyperglycemia. Cell energy metabolism detection demonstrated that GE could regulate the *miR-4429/*

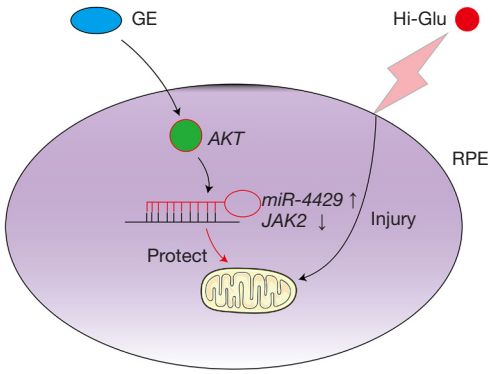

Figure 12 Research hypothesis. GE mediates the *miR-4429/JAK2* signaling axis through the *AKT* pathway to protect mitochondrial damage in RPE cells under hyperglycemia. GE, genipin; RPE, retinal pigment epithelial.

JAK2 signaling axis through the *AKT* pathway to protect mitochondrial function in RPE cells under hyperglycemia. Animal experiments were conducted to verify the molecular mechanism of the effect of GE on DR lesions in diabetic mice. Its specific regulatory molecular mechanism in RPE cells is shown in *Figure 12*.

The retinal pigment epithelium, as the monolayer of the most important nerve cells (photoreceptors) in the adjacent retinal tissue, plays an important role in the development of DR's characteristic vascular lesions (3). A study has shown that the retinal pigment epithelium is involved in early retinal microangiopathy (5). Oxidative stress and inflammatory responses are the main pathological changes of diabetic microangiopathy. As the organ and tissue with the highest oxygen consumption rate in the body, the retina is also more vulnerable to oxidative stress attack and thus cell damage (18). Studies have shown that oxidative stress promotes RPE cell damage mainly through affecting mitochondrial function (19). For example, mitochondrial energy metabolism changes, and the mitochondrial permeability transition pore opens, which releases *CYT C1* and causes apoptosis (20). As an effective antioxidant, GE has a certain protective effect on mitochondrial function. In this study, RPE cells were cultured under hyperglycemia, and the results showed that the cell activity was significantly decreased, the expression of *CYT C1* was significantly increased, mitochondrial function was significantly impaired, and mitochondrial permeability was increased. After the addition of GE, the activity of RPE cells increased, the expression of *CYT C1* and inflammatory response-related proteins decreased significantly, mitochondrial function recovered, and mitochondrial permeability decreased. These results suggest that GE can effectively protect mitochondrial function, protect cell activity, and inhibit the inflammatory responses of RPE cells under hyperglycemia.

In this study, we cultured RPE cells with high glucose and added GE and *AKT* signaling pathway inhibitors. The results showed that the activity of RPE cells was significantly inhibited after the inhibition of the *AKT* signaling pathway, and the expression of *CYT C1* and inflammatory response-related proteins was significantly increased. Meanwhile, mitochondrial energy metabolism was decreased, and mitochondrial permeability was significantly increased. These results showed that after the *AKT* signaling pathway was inhibited, the protective effect of GE on RPE cell activity, inflammatory responses, and mitochondrial function was significantly reduced in hyperglycemia. The *AKT* signaling pathway is closely related to the proliferation, differentiation, and apoptosis of cells in the body (21). A study has shown that the *AKT* signaling pathway is closely related to the progression of DR. Curcumin can protect against retinal damage in hyperglycemia through the *AKT*/mTOR signaling pathway (22). At the same time, a study has also shown that connective tissue growth factor can protect the functional activity of RPE cells through the *AKT* signaling pathway (23). Glycyrrhizin can protect RPE cells and retinal damage through the *AKT* signaling pathway (24). These results indicate that the *AKT* signaling pathway plays an important guiding role in the regulation of the functional activity of RPE cells. Meanwhile, changes in the expression of the *AKT* signaling pathway are closely related to changes in the mitochondrial function of RPE cells. A study has shown that pigment epithelial-derived factor (PEDF) can protect the mitochondrial function of RPE cells through the *AKT* signaling pathway (25). Lutein can protect cell activity through the *AKT* signaling pathway and effectively protect against mitochondrial energy metabolism changes (26). On this basis, this study suggests that GE mainly protects RPE cell activity, inhibits inflammatory responses, and protects mitochondrial function under hyperglycemia through the *AKT* signaling pathway.

As a classical signaling pathway, the *AKT* signaling pathway has numerous downstream proteins. The therapeutic effect of *AKT* on RPE cells needs to be clarified in terms of through which protein molecule it primarily achieves its therapeutic effect. With the development of

information technology, we believe that bioinformatics analysis can preliminarily identify the downstream proteins mainly regulated by the *AKT* signaling pathway during GE treatment of RPE cells. In this study, the differentially expressed genes after GE treatment of RPE cells were screened through databases, and the downstream proteins of the *AKT* signaling pathway were obtained through the KEGG website. After the intersection of differentially expressed genes and the *AKT* signaling pathway, the results showed that RPRL and *JAK2* were the downstream molecules of differentially expressed *AKT*. RPRL is closely related to the development of breast system diseases (13). *JAK2* is closely related to the body's inflammatory response and mitochondrial function damage (14). A study has suggested that interleukin-2 (IL-2) can regulate the expression of inflammatory cytokines in RPE cells through *JAK2* and reduce the activity of RPE cells (27). Glycosylated serum protein can promote the secretion of inflammatory cytokines (IL-8) and the expression of MCP-1 by RPE cells through *JAK2*, thus affecting the function and activity of RPE cells (28). At the same time, a study has shown that the expression level of *JAK2* is closely related to mitochondrial function, and extracellular IL-6 can affect the physiological function of intracellular mitochondria by regulating the expression of *JAK2* (29). High glucose stimulation can cause mitochondrial dysfunction by promoting the expression of *JAK2* (30). On this basis, this study suggests that GE may regulate the expression of *JAK2* through the *AKT* pathway to protect RPE cells from injury under hyperglycemic conditions. How does the *AKT* protein regulate *JAK2* expression? This study suggests that *AKT* may exert a certain influence on JAK expression by regulating the expression changes of intracellular miRNAs.

MiRNAs, as a class of non-coding RNAs with about 18–22 nucleotide sequences, are closely related to the functional expression of body cells (31). In order to identify the miRNAs with targeted regulation by *JAK2*, this study retrieved and intersected data from the TargetScan, miRDB, and DIANA databases, and finally obtained *miR-4429* as a miRNA that may have a targeted relationship with *JAK2* mRNA. *MiR-4429* has been thoroughly studied by previous researchers as a recognized tumor suppressor gene. A study has shown that *miR-4429* exists as a tumor suppressor in the progression of various malignant tumors. In glioblastoma cells, inhibiting the expression of *miR-4429* can accelerate the growth of cancer cells (32). *MiR-4429* is downregulated in cervical cancer and can target the DNA double-strand break repair protein (RAD51) to sensitize cervical cancer cells to radiotherapy (33). *MiR-4429* inhibits cervical cancer cell proliferation, migration, and invasion by targeting FOXM1. Long non-coding RNA (lncRNA) PSMA3-AS1 promotes the migration and invasion of colorectal cancer cells by regulating *miR-4429* (34). At the same time, the results also showed that *miR-4429* was also closely related to intracellular energy metabolism. Overexpression of *miR-4429* can reduce glucose consumption, lactic acid production, and the protein levels of PKM2 and HK2 in breast cancer cells, as well as increase the inhibition rate of cell proliferation and decrease the number of clones, suggesting that overexpression of *miR-4429* can inhibit the glycolysis, lysis, proliferation, and clone formation of breast cancer cells (35,36). However, whether *miR-4429* has regulatory effects on cell activity, function, and mitochondrial energy metabolism in high glucose-induced RPE cell damage has not been reported before. The results of this study showed that when *miR-4429* was overexpressed during GE treatment, the activity of RPE cells was significantly increased, while the expression of inflammatory factors was significantly decreased, and the detection results of WB and mitochondrial energy metabolism showed that the mitochondrial energy metabolism function was significantly improved. Meanwhile, the expression of *JAK2* was also significantly increased. However, after *JAK2* inhibition during GE treatment, the activity of RPE cells was significantly increased, while the expression of inflammatory factors was significantly decreased, and the results of WB and mitochondrial energy metabolism showed that the mitochondrial energy metabolism function was significantly improved. Additionally, the expression of *miR-4429* had no significant effect. On this basis, the dual luciferase reporter assay was used to further prove that *miR-4429* has a targeted binding effect with *JAK2*. Therefore, this study suggested that GE could protect RPE cells from injury in hyperglycemia through the *miR-4429*/*JAK2* signaling axis. In order to further clarify the regulatory relationship between the *AKT* signaling pathway and the *miR-4429*/*JAK2* signaling axis, this study further compared and analyzed the changes in the function and metabolism of cells after adding *AKT* inhibitor and overexpression/knockdown of *miR-4429*. The results showed that the expression of *miR-4429* was significantly reduced after adding *AKT* inhibitor, while there was no significant difference in the expression of *AKT* after overexpression/knockdown of *miR-4429*, suggesting that *miR-4429* is a downstream molecule of *AKT*. In order to further verify the therapeutic mechanism of GE for DR,

this study established a diabetic mouse model to further clarify the therapeutic effect of GE on DR and changes in molecular expression during treatment.

Conclusions

In this study, bioinformatics analysis was used to predict the molecular mechanism of GE in the treatment of RPE cell damage caused by high glucose. Through the addition of *AKT* inhibitors, knockdown/overexpression by lentivirus infection, and other methods, we demonstrated that GE can regulate the expression changes of the *miR-4429/JAK2* signaling axis through the *AKT* signaling pathway, thus realizing the protective effect on the function, activity, and mitochondrial damage of RPE cells under hyperglycemia.

Acknowledgments

Funding: This study was funded by Science and Technology Joint Guidance Program of Qiqihar, China (No. LHYD-202012) and Basic Scientific Research Business Expenses, Research Project of Heilongjiang Provincial Undergraduate College (No. 2019-KYYWF-1253).

Footnote

Reporting Checklist: The authors have completed the ARRIVE reporting checklist. Available at https://atm.amegroups.com/article/view/10.21037/atm-22-2219/rc

Data Sharing Statement: Available at https://atm.amegroups.com/article/view/10.21037/atm-22-2219/dss

Conflicts of Interest: All authors have completed the ICMJE uniform disclosure form (available at https://atm.amegroups.com/article/view/10.21037/atm-22-2219/coif). All authors report that this study was funded by Science and Technology Joint Guidance Program of Qiqihar, China (No. LHYD-202012) and Basic Scientific Research Business Expenses, Research Project of Heilongjiang Provincial Undergraduate College (No. 2019-KYYWF-1253). The authors have no other conflicts of interest to declare.

Ethical Statement: The authors are accountable for all aspects of the work in ensuring that questions related to the accuracy or integrity of any part of the work are appropriately investigated and resolved. The study was conducted in accordance with the Declaration of Helsinki (as revised in 2013). Animal experiments were performed under a project license (No. QMU-AECC-2021-244) granted by Animal Ethical Committee of Qiqihar Medical University, in compliance with national guidelines for the care and use of animals.

References

1. Qi X, Mitter SK, Yan Y, et al. Diurnal Rhythmicity of Autophagy Is Impaired in the Diabetic Retina. Cells 2020;9:905.
2. Schmidt-Erfurth U, Garcia-Arumi J, Bandello F, et al. Guidelines for the Management of Diabetic Macular Edema by the European Society of Retina Specialists (EURETINA). Ophthalmologica 2017;237:185-222.
3. Potilinski MC, Ortíz GA, Salica JP, et al. Elucidating the mechanism of action of alpha-1-antitrypsin using retinal pigment epithelium cells exposed to high glucose. Potential use in diabetic retinopathy. PLoS One 2020;15:e0228895.
4. Dolinko AH, Chwa M, Atilano SR, et al. African and Asian Mitochondrial DNA Haplogroups Confer Resistance Against Diabetic Stresses on Retinal Pigment Epithelial Cybrid Cells In Vitro. Mol Neurobiol 2020;57:1636-55.
5. Kim DY, Kang MK, Lee EJ, et al. Eucalyptol Inhibits Amyloid-β-Induced Barrier Dysfunction in Glucose-Exposed Retinal Pigment Epithelial Cells and Diabetic Eyes. Antioxidants (Basel) 2020;9:1000.
6. Zhang C, Xie H, Yang Q, et al. Erythropoietin protects outer blood-retinal barrier in experimental diabetic retinopathy by up-regulating ZO-1 and occludin. Clin Exp Ophthalmol 2019;47:1182-97.
7. Tian JS, Zhao L, Shen XL, et al. 1H NMR-based metabolomics approach to investigating the renal protective effects of Genipin in diabetic rats. Chin J Nat Med 2018;16:261-70.
8. Li F, Song L, Chen J, et al. Effect of genipin-1-β-d-gentiobioside on diabetic nephropathy in mice by activating AMP-activated protein kinase/silencing

information regulator-related enzyme 1/nuclear factor-κB pathway. J Pharm Pharmacol 2021;73:1201-11.
9. Zhang J, Wang YN, Jia T, et al. Genipin and insulin combined treatment improves implant osseointegration in type 2 diabetic rats. J Orthop Surg Res 2021;16:59.
10. Qiu W, Zhou Y, Jiang L, et al. Genipin inhibits mitochondrial uncoupling protein 2 expression and ameliorates podocyte injury in diabetic mice. PLoS One 2012;7:e41391.
11. Zhao H, Wang R, Ye M, et al. Genipin protects against H2O2-induced oxidative damage in retinal pigment epithelial cells by promoting Nrf2 signaling. Int J Mol Med 2019;43:936-44.
12. Lai JY. Biocompatibility of genipin and glutaraldehyde cross-linked chitosan materials in the anterior chamber of the eye. Int J Mol Sci 2012;13:10970-85.
13. McKinnie SMK, Wang W, Fischer C, et al. Synthetic Modification within the "RPRL" Region of Apelin Peptides: Impact on Cardiovascular Activity and Stability to Neprilysin and Plasma Degradation. J Med Chem 2017;60:6408-27.
14. Tan JK, Ma XF, Wang GN, et al. LncRNA MIAT knockdown alleviates oxygen-glucose deprivation-induced cardiomyocyte injury by regulating JAK2/STAT3 pathway via miR-181a-5p. J Cardiol 2021;78:586-97.
15. Wei J, Wang Z, Wang W, et al. Oxidative Stress Activated by Sorafenib Alters the Temozolomide Sensitivity of Human Glioma Cells Through Autophagy and JAK2/STAT3-AIF Axis. Front Cell Dev Biol 2021;9:660005.
16. Garcia-Ramírez M, Hernández C, Ruiz-Meana M, et al. Erythropoietin protects retinal pigment epithelial cells against the increase of permeability induced by diabetic conditions: essential role of JAK2/PI3K signaling. Cell Signal 2011;23:1596-602.
17. Platania CBM, Maisto R, Trotta MC, et al. Retinal and circulating miRNA expression patterns in diabetic retinopathy: An in silico and in vivo approach. Br J Pharmacol 2019;176:2179-94.
18. Yu B, Ma J, Li J, et al. Mitochondrial phosphatase PGAM5 modulates cellular senescence by regulating mitochondrial dynamics. Nat Commun 2020;11:2549.
19. Somasundaran S, Constable IJ, Mellough CB, et al. Retinal pigment epithelium and age-related macular degeneration: A review of major disease mechanisms. Clin Exp Ophthalmol 2020;48:1043-56.
20. Brown EE, DeWeerd AJ, Ildefonso CJ, et al. Mitochondrial oxidative stress in the retinal pigment epithelium (RPE) led to metabolic dysfunction in both the RPE and retinal photoreceptors. Redox Biol 2019;24:101201.
21. Chen Q, Tang L, Xin G, et al. Oxidative stress mediated by lipid metabolism contributes to high glucose-induced senescence in retinal pigment epithelium. Free Radic Biol Med 2019;130:48-58.
22. Qin D, Jiang YR. Tangeretin Inhibition of High-Glucose-Induced IL-1β, IL-6, TGF-β1, and VEGF Expression in Human RPE Cells. J Diabetes Res 2020;2020:9490642.
23. Zha X, Xi X, Fan X, et al. Overexpression of METTL3 attenuates high-glucose induced RPE cell pyroptosis by regulating miR-25-3p/PTEN/Akt signaling cascade through DGCR8. Aging (Albany NY) 2020;12:8137-50.
24. Wang T, Zhang Z, Song C, et al. Astragaloside IV protects retinal pigment epithelial cells from apoptosis by upregulating miR-128 expression in diabetic rats. Int J Mol Med 2020;46:340-50.
25. Su CC, Chan CM, Chen HM, et al. Lutein inhibits the migration of retinal pigment epithelial cells via cytosolic and mitochondrial Akt pathways (lutein inhibits RPE cells migration). Int J Mol Sci 2014;15:13755-67.
26. Shukal D, Bhadresha K, Shastri B, et al. Dichloroacetate prevents TGFβ-induced epithelial-mesenchymal transition of retinal pigment epithelial cells. Exp Eye Res 2020;197:108072.
27. Parmar T, Parmar VM, Arai E, et al. Acute Stress Responses Are Early Molecular Events of Retinal Degeneration in Abca4-/-Rdh8-/- Mice After Light Exposure. Invest Ophthalmol Vis Sci 2016;57:3257-67.
28. Shen CH, Hsieh CC, Jiang KY, et al. AUY922 induces retinal toxicity through attenuating TRPM1. J Biomed Sci 2021;28:55.
29. Li R, Wen R, Banzon T, et al. CNTF mediates neurotrophic factor secretion and fluid absorption in human retinal pigment epithelium. PLoS One 2011;6:e23148.
30. Chen X, Sun R, Yang D, et al. LINC00167 Regulates RPE Differentiation by Targeting the miR-203a-3p/SOCS3 Axis. Mol Ther Nucleic Acids 2020;19:1015-26.
31. Qi T, Jing R, Wen C, et al. Interleukin-6 promotes migration and extracellular matrix synthesis in retinal pigment epithelial cells. Histochem Cell Biol 2020;154:629-38.
32. Duncan RS, Rohowetz L, Vogt A, et al. Repeat exposure to polyinosinic:polycytidylic acid induces TLR3 expression via JAK-STAT signaling and synergistically potentiates NFκB-RelA signaling in ARPE-19 cells. Cell Signal 2020;66:109494.
33. Jing R, Qi T, Wen C, et al. Interleukin-2 induces

extracellular matrix synthesis and TGF-β2 expression in retinal pigment epithelial cells. Dev Growth Differ 2019;61:410-8.
34. Patel AK, Syeda S, Hackam AS. Signal transducer and activator of transcription 3 (STAT3) signaling in retinal pigment epithelium cells. JAKSTAT 2013;2:e25434.
35. Li R, Maminishkis A, Banzon T, et al. IFN{gamma} regulates retinal pigment epithelial fluid transport. Am J Physiol Cell Physiol 2009;297:C1452-65.
36. Kucharska J, Del Río P, Arango-Gonzalez B, et al. Cyr61 activates retinal cells and prolongs photoreceptor survival in rd1 mouse model of retinitis pigmentosa. J Neurochem 2014;130:227-40.

(English Language Editor: C. Betlazar-Maseh)

Cite this article as: Xu W, Chen Q, Zhang X, Zhao Y, Wu S, Yang C, Liu Y, Liang L, Jia D, Li C, Fan L, Shi Y. Genipin protects against mitochondrial damage of the retinal pigment epithelium under hyperglycemia through the *AKT* pathway mediated by the *miR-4429/JAK2* signaling axis. Ann Transl Med 2022;10(10):587. doi: 10.21037/atm-22-2219

